



Research Article

Synthesis of *Aloe vera*-conjugated silver nanoparticles for use against multidrug-resistant microorganisms

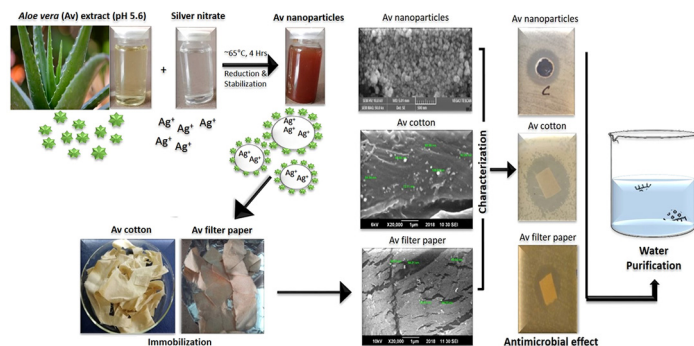
Hammad Arshad ^{a,b}, Misbah Saleem ^a, Usman Pasha ^a, Saima Sadaf ^{a,*}

^a School of Biochemistry & Biotechnology, University of the Punjab, Lahore 54590, Pakistan

^b Department of Biology, Lahore Garrison University, Lahore, Pakistan



GRAPHICAL ABSTRACT



ARTICLE INFO

Article history:

Received 28 March 2021

Accepted 10 November 2021

Available online 17 November 2021

Keywords:

Aloe vera

Antimicrobials

Green synthesis

Multidrug resistance

Silver nanoparticles

ABSTRACT

Background: The emergence of multidrug-resistant (MDR) microorganisms is one of the biggest and most challenging public health issues drawing considerable attention of the scientific community. Here, we present an easy, one-step, inexpensive and ecofriendly/biologically mediated synthesis of *Aloe vera*-conjugated silver nanoparticles (Av-AgNPs) where the aqueous plant extract acts as a reducing and stabilizing agent and the resultant conjugate exhibits remarkable potential to limit/inhibit the growth of MDR pathogens.

Results: The nanosynthesis concluded in 4–6 h at 65°C and was followed by detailed characterization of the bioconjugated Av-AgNPs (with and without fabrication on cellulosic materials i.e., cotton fabric and filter paper) using a combination of UV–visible spectroscopy, Fourier transform infrared spectroscopy (FTIR), scanning electron microscopy (SEM), x-ray diffraction (XRD) and inductively coupled plasma optical emission spectroscopy (ICP-OES). The so-characterized NPs showed growth inhibitory effects on multiple strains including the Gram-positive *Staphylococcus aureus*, Gram-negative *Escherichia coli* (*E. coli*), *Acinetobacter baumannii* (*A. baumannii*), *Pseudomonas aeruginosa* (*P. pseudomonas*) and, more importantly, the fungus *Candida albicans* (*C. albicans*), when analyzed using the Kirby-Bauer method. A notable reduction in the colony-forming unit (CFU) counts of the *E. coli* (present in contaminated drinking water) was also observed when the filter paper encrusted with Av-AgNPs was applied as a filtration material.

Abbreviations: Av, *Aloe vera*; FTIR, Fourier transform infrared spectroscopy; MDR, Multidrug resistance; WHO, World Health Organization; XRD, X-ray diffraction; SEM, Scanning electron microscopy; NPs, Nanoparticles; AgNPs, Silver nanoparticles.

Peer review under responsibility of Pontificia Universidad Católica de Valparaíso

* Corresponding author.

E-mail address: saima.sbb@pu.edu.pk (S. Sadaf).

<https://doi.org/10.1016/j.ejbt.2021.11.003>

0717-3458/© 2021 Pontificia Universidad Católica de Valparaíso. Production and hosting by Elsevier B.V.

This is an open access article under the CC BY-NC-ND license (<http://creativecommons.org/licenses/by-nc-nd/4.0/>).

Conclusions: In conclusion, the biofabricated Av-AgNPs are easy to synthesize and are a cost-effective alternative to inorganic AgNPs, with considerable antimicrobial activity, deserving further investigations for biomedical applications.

How to cite: Arshad H, Saleem M, Pasha U, et al. Synthesis of *Aloe vera*-conjugated silver nanoparticles for use against multidrug-resistant microorganisms. *Electron J Biotechnol* 2022;55. <https://doi.org/10.1016/j.ejbt.2021.11.003>

© 2021 Pontificia Universidad Católica de Valparaíso. Production and hosting by Elsevier B.V. This is an open access article under the CC BY-NC-ND license (<http://creativecommons.org/licenses/by-nc-nd/4.0/>).

1. Introduction

Owing to an increasingly high mortality rate and associated morbidity, second-/third-line broad-spectrum antibiotic-resistant microorganisms pose an alarming threat to the public and tertiary healthcare systems globally [1]. According to the WHO report (2019), over 700,000 people die each year due to the inefficacy of antimicrobials against the rapidly evolving resistant strains of bacteria, thereby exposing the immune-compromised subjects (cancer patients and others) at an even greater risk of adverse outcomes and treatment complications [2,3,4]. This advocates the need for repeated surveillance in the healthcare settings and devising innovative strategies for improved management of this complex, multifaceted challenge i.e., counteracting/eradicating the multidrug-resistant (MDR) microorganisms without adverse, long-term treatment effects.

Recent advances and accumulating evidence suggest that nanotechnology-driven revolutions exploiting the use of metal-based nanosized particles may eliminate the bacterial infections, combat the spread of resistant microbes and serve as a promising alternative to the conventional antibiotics [5,6,7]. Among the metallic nanoparticles [e.g., silver (Ag), zinc (Zn), copper (Cu) and gold (Au)], silver nanoparticles (AgNPs) are at the forefront of research due to their antimicrobial and anticancer properties, potential usage in heavy metal scavenging, catalytic activity against azo dyes, etc. [8,9]. Ag in its elemental form is toxic and can kill microbes quite effectively. Coupling/conjugation between the AgNPs results in a severalfold increase in the bactericidal properties of Ag, due primarily to the high surface area-to-volume ratio of the NPs, allowing enhanced interactions and accessibility to the targeted microbes [8,10,11,12,13].

For the synthesis of NPs, a wide range of physical (top-down approach) and chemical (bottom-up approach) methods have conventionally been employed. Whereas the physical methods are time consuming and implicate expensive instrumentation and a high amount of energy, the chemical methods quick but involve the use of toxic chemicals and produce harmful by-products that negatively affect the natural ecosystem [9]. Owing to these limitations/drawbacks, currently, the most attractive method to produce NPs entails the use of biological sources such as microorganisms (bacteria, fungi, algae) or plant-based materials (roots, shoots, leaves, fruit peels), being both rapid/cost-effective and eco-friendly/biocompatible [14,15,16,17].

Several research groups have reported the synthesis of Zn-, Ag-, Au-, Cu- and Ag-Au bimetallic NPs, ranging in size from 10 to 80 nm with spherical, cubic, rectangular, polyhedron or even mixed morphologies, using ethanolic or aqueous extracts from different parts of the plants such as *Catharanthus roseus*, *Azadirachta indica*, *Boerhaavia diffusa*, *Terminalia fagifolia*, *Butea monosperma*, *Rosemary*, *Pulicaria undulata*, *Phyllanthus urinaria*, *Pouzolzia zeylanica* and *Scoparia dulcis*, to name a few [18,19,20,21,22,23,24]. *Aloe vera* (Av), a member of the Liliaceae family, is yet another interesting medicinal plant, long known for its anti-bacterial, anti-inflammatory, anti-arthritic, and burn-/wound-healing properties.

Its gel and leaf extracts are rich in nutrients and contain over 200 active compounds including simple/complex polysaccharides, amino acids, proteins, enzymes, terpenoids, flavonoids, saponins, minerals, vitamins, phenols and other metabolites, which endow Av with unique features allowing a broad spectrum of applications [25]. These phyto-constituents (more specifically, polyphenols, proteins and organic acids), while working synergistically, may act as reducing and capping agents for the surface functionalization of metallic NPs [26,27].

By considering the aforementioned points, we, in the present study, have coupled the 'biocidal properties of Av and Ag' in the form of uniform-sized NPs by employing an easy, one-step, chemical-free approach and have monitored the biocidal effect of the biofabricated Av-AgNPs over the clinically isolated MDR strains of Gram-positive/Gram-negative bacteria and the fluconazole-resistant *Candida albicans* (*C. albicans*) (which have largely remained unexplored). In contrast to most of the other studies wherein the use of additional chemicals and long reaction time (24 up to 72 h) has been described for Ag⁺ reduction, capping, or completion of the synthesis process [26,28,29,30,31], the method presented in this study is a one-step procedure for producing NPs that are stable for months with little or no contamination and agglomeration. The findings of the present research study provide further evidence that phyto/biologically mediated synthesis of NPs is quick, safe/eco-friendly and easy to scale up and also that the Av-AgNPs (with/without fabrication over cellulosic materials such as cotton fiber/filter paper) can limit/inhibit the growth of MDR pathogens, opening new avenues for potential biomedical applications.

2. Material and methods

2.1. Materials and preparation of stock solutions

Silver nitrate salt (AgNO₃; 99.9%) was procured from Sigma Aldrich, USA (Cat. No. 209139-25G). Fresh leaves from the Av plant were collected from a local nursery of Lahore, whereas clinically isolated fungal (*C. albicans*) and bacterial strains including Gram-positive *Staphylococcus aureus* (*S. aureus*) and Gram-negative *Escherichia coli* (*E. coli*), *Acinetobacter baumannii* (*A. baumannii*) and *Pseudomonas aeruginosa* (*P. aeruginosa*) were obtained from the Pathology Lab. of Combined Military Hospital (CMH), Lahore, Pakistan.

A 10 mM stock solution of the metal precursor, i.e., AgNO₃, was prepared in deionized water and stored in an amber-colored bottle to prevent photooxidation. For the preparation of the Av extract, fresh Av leaves (10 g) were thoroughly washed with distilled water three times, finely sliced into small pieces, boiled in 100 mL distilled water for 10 minutes, cooled at room temperature, filtered using Whatman filter paper (grade 1) and stored at 4°C, until use. For long-term storage, the green-colored Av-extract was filter-sterilized through 0.45 μm Amicon™ filters and placed at 4°C.

2.2. Synthesis of Av-AgNPs

The synthesis of Av-AgNPs was carried out as described earlier [32], with some modifications. Briefly, 10% Av extract (natural pH:5.5–5.6) was mixed with 10 mM AgNO₃ solution in different ratios, i.e., 9:1, 8:2 and 7:3, under constant, slow-speed stirring on a magnetic stir plate. To optimize the quick and stable formation of NPs, the temperature and incubation time was modulated between 25°C (room temperature) and 65°C, for 1–48 h of extended duration. During incubation, the change in color from faint yellow to dark brown was monitored, following which the synthesized Av-AgNPs were centrifuged (6000 rpm; 15 min) and washed with deionized water (3 times) to remove impurities and prevent subsequent agglomeration.

The optimized synthesis protocol was thereafter used for Av-mediated fabrication of AgNPs onto small (2–4 inches), thoroughly washed (twice with distilled water, once with 70% ethanol), oven dried (45–50°C) cellulosic materials, more specifically, white-colored cotton fabric and grade 2 Whatman filter paper (PN: 1002-055). The color change was observed within 4 h, following which the fabric and the filter paper were washed with distilled water (3x) and 70% ethanol (1x) and oven dried at 50°C for 2 h to remove water contents and ethanol. The cotton fabric and filter paper, similarly impregnated with 10 mM AgNO₃ and 10% Av extract (natural pH) each, were used as control.

2.3. Characterization of Av-AgNPs and biofabricated cellulosic material

The synthesis of Av-AgNPs was characterized using a series of techniques. More importantly, the change in color due to the reduction of Ag⁺ was monitored both visually and by using ultraviolet–visible (UV–vis) spectrophotometry (SPECORD 200, Germany) over the spectral range of 300–900 nm, for different time intervals (1–24 h) against distilled water, used as blank. To identify the possible phytochemicals involved in the reduction and capping during the synthesis of Av-AgNPs, Fourier transform infrared spectroscopy (FTIR; Nicolet FTIR 6700, Thermo Scientific, USA) was performed.

The size and morphology of Av-AgNPs and biofabricated cotton (Av-Ag-Cot) and filter paper (Av-Ag-FP) were analyzed using scanning electron microscopy (SEM). Briefly, an aqueous suspension of Av-AgNPs was drop-cast on a clean silicon wafer attached with carbon tape and observed under JSM-6490A JEOL electron microscope operated at low accelerating voltage (10 kV). In the case of Av-Ag-Cot and Av-Ag-FP, the samples were placed directly on the carbon tape under a SEM operated at 6 kV, and the images were captured at different ranges of magnifications, for detailed analysis.

For x-ray diffraction (XRD) analysis, the heat-dried Av-AgNP (at 50°C incubator) sample was evenly spread over the glass holder and analyzed on a Bruker D-8-Advance instrument; XRD scan ranging between 20 and 60 with θ scan of 2degrees. This was followed by plotting of the graph using Origin Pro 2020 software.

Finally, for inductively coupled plasma optical emission spectroscopic analysis (ICP-OES), the test (Av-AgNPs, Av-Ag-Cot, Av-Ag-FP) and control samples (distilled water, filtrate) were prepared by the wet acidic digestion method [33]. Briefly, 5 mL of 50% nitric acid and 10 mL of 30% H₂O₂ were added (2 mL at a time in different intervals, until all the matter was digested and solubilized at 120°C). The samples were filtered and diluted up to 100 mL with deionized water, and the concentration of Ag in each sample was measured on a Perkin Elmer 7000-W, ICP-OES analyzer, at 328.068 nm against five different aqueous standards (1–5 ppm).

2.4. Antimicrobial activity assessment

The antimicrobial activity testing was carried out by the Kirby-Bauer agar disc- and/or agar well diffusion methods, using Muller

Hinton Agar (MHA) [34]. Sterilized/autoclaved (15 min at 15 lb/inch² pressure and 121°C temperature) agar medium was poured in Petri plates and left to solidify under aseptic conditions. Wells were made in agar by using a pipette tip of 0.5 cm diameter. Overnight grown cultures of Gram-positive and Gram-negative MDR bacteria and fungus *C. albicans* were diluted and uniformly spread over the media, with an approximate concentration of 1×10^8 colony-forming units per milliliter [CFU/mL; OD₆₀₀ ~0.1]. The test samples [Av-AgNPs (100, 200 µg) and Av-Ag-Cot, Av-Ag-FP (tested as 5 ± 1 mm pieces)] were introduced into agar wells or agar plates and left undisturbed for 10 min followed by the incubation of the plates at 37°C, for 18–24 h. The antimicrobial activity was measured by analyzing the zones of inhibition (ZOI) formed around the test samples. All the samples were tested at least in triplicate under aseptic conditions, and the results are presented as average ± standard deviation (SD).

2.5. Estimating the minimum inhibitory concentration (MIC) and the minimum bactericidal concentration (MBC)

For determining the MIC, serially diluted Av-AgNPs (25–400 µg/mL) were added in sterile test tubes containing nutrient broth (N-broth). The test organism (OD₆₀₀ = 0.1) was inoculated in each tube and incubated at 37°C for 24 h in a shaking incubator (120 rpm); a test tube without Av-AgNPs was used as a negative control for each pathogen. The MIC was calculated as the minimum concentration that inhibited the 98% growth of pathogens, while the MBC was equal to or more than the MIC and calculated as the concentration that diminished the inoculated viable cells by ≥99.9%. The MIC and MBC were confirmed by serial dilutions and plating of cultures on MHA (incubated at 37°C for 18–24 h), and by CFU/mL counts.

2.6. Efficacy of Av-AgNPs in treating contaminated water

The efficacy of Av-AgNPs to remove/reduce *E. coli*, mostly found in fecal contaminated water, was tested using the filter paper encrusted with Av-AgNPs (Av-Ag-FP). Autoclaved nutrient broth (10 mL) was inoculated with a single colony of *E. coli* and incubated overnight at 37°C with constant shaking (120 rpm). The overnight culture was diluted with normal saline until the OD₆₀₀ value reached 0.1 (equivalent to ~10⁸ CFU/mL), following which the same was filtered through Av-Ag-FP. The filtrate was analyzed for the presence of *E. coli* both by OD₆₀₀ measurements and reduction in the CFU/mL count, calculated using the formula:

% Bacterial Reduction = $[(X-Y)/X] \times 100$ Where X = initial number of CFUs in the sample and Y = number of CFUs after filtration

Filter papers impregnated with AgNO₃ and water were used as positive and negative controls, respectively; those carrying 10% immobilized Av were also tested for bacterial reduction, found in the contaminated water.

3. Results

3.1. Synthesis of Av-AgNPs and SEM analysis

Av-AgNPs were successfully synthesized by mixing the AgNO₃ and Av stock solutions in a 7:3 ratio, under constant, gentle stirring and heating conditions (temperature, 65 ± 5°C); the scheme of NP formation is shown in Fig. 1. The synthesized Av-AgNPs showed a change in color from light yellow to dark brown (Fig. 2A) within the initial 60 min, but completion of the reduction reaction was observed at 4–6 h post-incubation. The UV–Vis spectrum (Fig. 2B) showed the highest absorbance of Av-AgNPs at 425 nm; peaks with similar intensities in this region were absent in the case of AgNO₃ solution and/or the Av extract, thus indicating the pres-

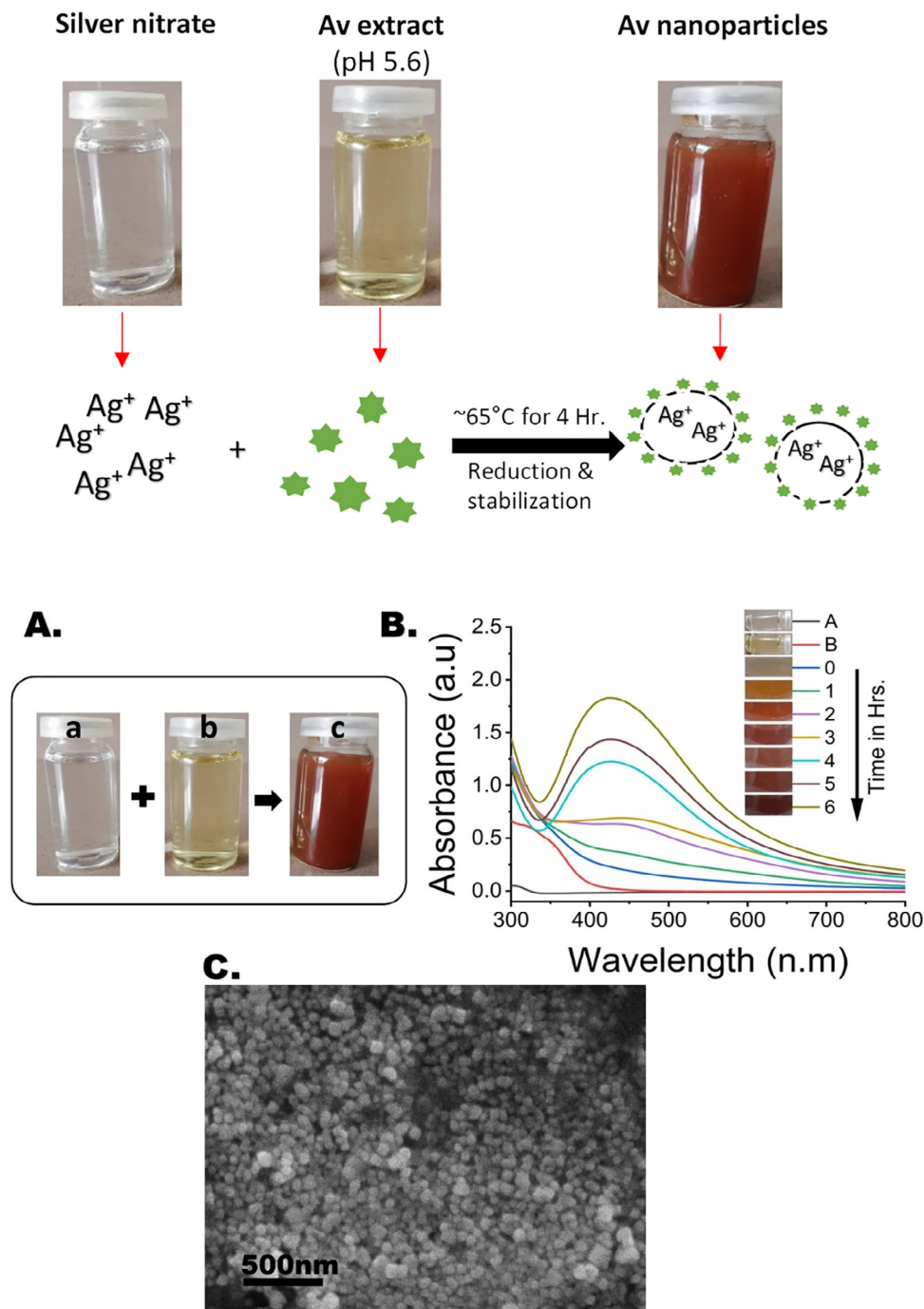


Fig. 2. Synthesis, UV-visible spectroscopy and electron microscopy of Av-AgNPs. (A) Soln. A (a; 10 mM AgNO_3) and Soln. B (b; 10% w/v Aloe vera extract) mixed and heated to synthesize Av-AgNPs (c; Av conjugated AgNPs). (B) UV-visible spectroscopy confirmed the surface plasmon resonance in Av-AgNPs at 425 nm after 3 h while there was no absorbance observed in AgNO_3 and Av extract. (C) Scanning electron microscopy depicts the spherical nature of Av-AgNPs.

ence of AgNPs in the reaction mixture. SEM analysis revealed that the synthesized NPs exhibit a spherical shape (Fig. 2C) and are in the 30–80 nm size range without any noticeable particle aggregation/agglomeration. A similar configuration was observed over the cotton fabric and the filter paper impregnated with NPs i.e., Av-Ag-Cot and Av-Ag-FP (shown by arrows; Fig. 3A).

3.2. Characterization of the AgNPs – FTIR, XRD and ICP-OES analysis

The FTIR spectrum indicated the presence of phytochemical head groups on the synthesized Av-AgNPs (Fig. 4A). Whereas the Av extract showed the maximum transmittance at 3254.1 cm^{-1} ,

2123 cm^{-1} and 1631.78 cm^{-1} , the Av-AgNPs displayed the same at 3271.5 cm^{-1} , 2107 cm^{-1} and 1632.62 cm^{-1} . The XRD data (Fig. 4B) presented the characteristic diffraction patterns with a distinctive value of $2\theta = 38.2^\circ$ and 45.6° , which relates to the (1 1 1) and (2 0 0) planes. The observed Bragg's reflection matching to (1 1 1) and (2 0 0) may be indexed based on the face-centric cubic (FCC) structure of the silver NPs [27,35]. The analysis provided an insight that the NPs are silver in nature and exhibit crystalline structure.

Furthermore, the ICP-OES analysis confirmed the presence of 56 mg/g Ag metal (5.6% w/w) in the synthesized Av-AgNPs and the attachment of Av-AgNPs on cellulosic materials (Fig. 3B), with

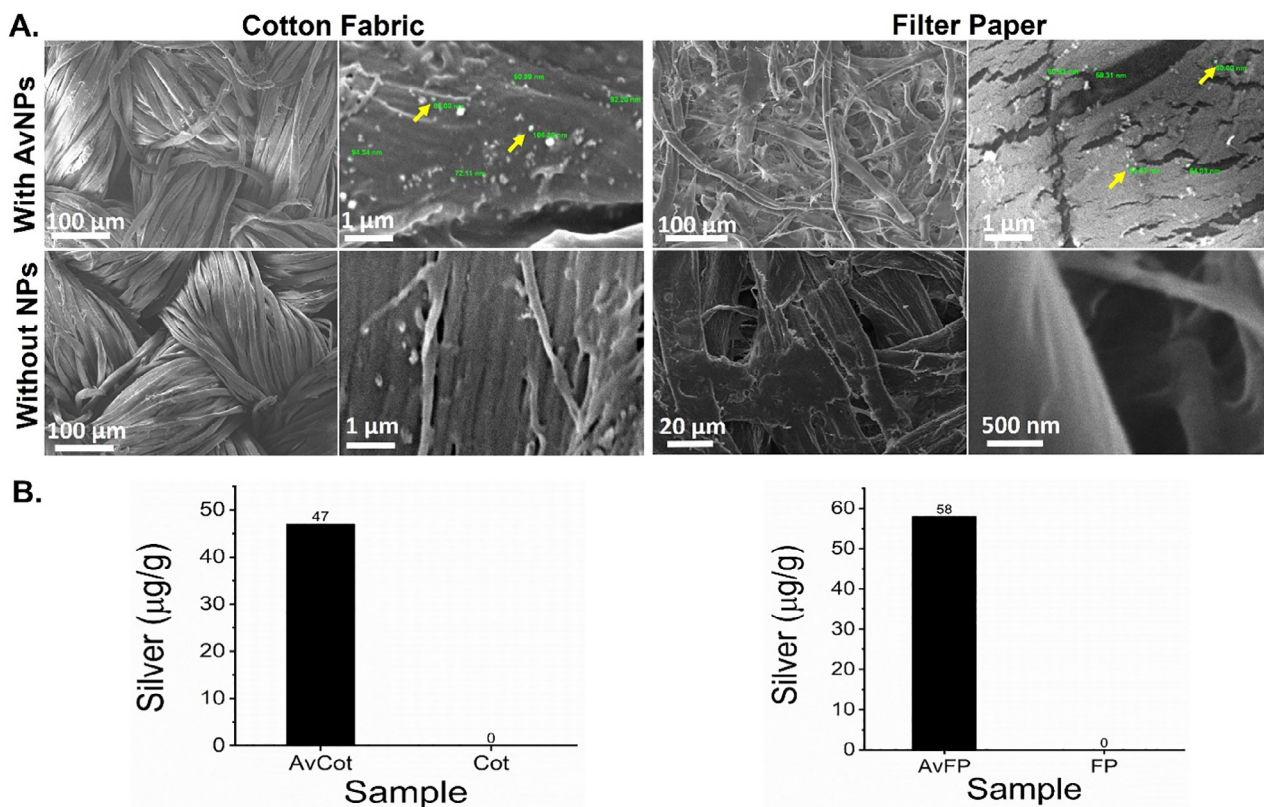


Fig. 3. Electron microscopy and quantification of silver content in cellulosic materials. SEM micrographs showing the presence of Av-AgNPs (yellow arrows) on cotton and filter paper in comparison with simple materials without NPs (A). The amount of Ag ions in Av-Ag-Cot and Av-Ag-FP was measured by ICP-OES (B).

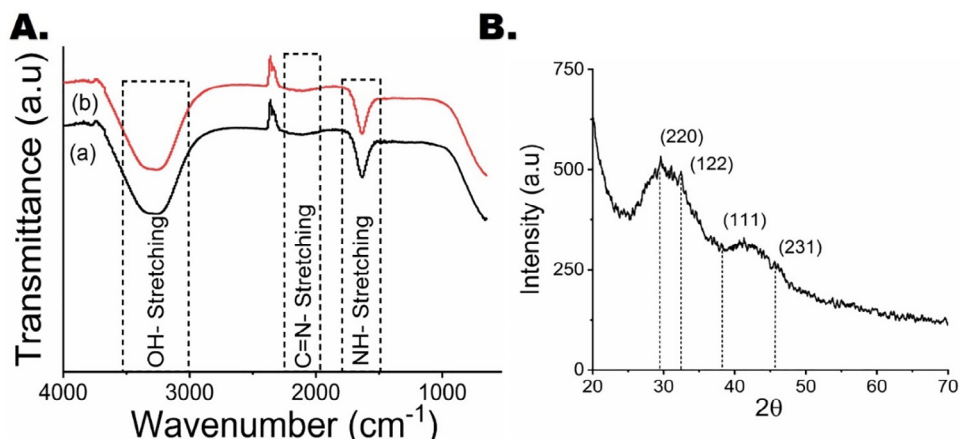


Fig. 4. Fourier transform infrared spectroscopy and X-ray diffraction analysis of Av-AgNPs. (A) FTIR confirmed the presence of similar bond stretching (OH-, NH- and C=N-) in Av-AgNPs (b) as observed in the Av extract (a). (B) XRD data showing the presence of face-centered cubic structures of Av-AgNPs.

Ag contents being equivalent to 47 µg/g of cotton and 58 µg/g of filter paper, respectively.

3.3. Antimicrobial assay

Antimicrobial activities of both the aqueous suspensions of Av-AgNPs and the immobilized NPs, Av-Ag-Cot and Av-Ag-FP, were tested against *C. albicans*, and the MDR strains of Gram-positive/negative bacteria (Table 1); the results are summarized in Fig. 5. For AvNPs, the reduction in the microbial growth was measured using a well diffusion method and all pathogens were found to be sensitive to silver ions (AgNO₃) and Av-AgNPs. However, with Av extract only, no notable reduction in growth could be recorded.

The *S. aureus* (Gram-positive) was found to be resistant, whereas the Gram-negative *E. coli*, *P. pseudomonas*, *A. baumannii* and *C. albicans* were found to be sensitive, to 100 and 200 µg/g concentrations of Av-AgNPs (Fig. 6). Interestingly, the biofabricated Av-Ag-Cot and Av-Ag-FP also showed significant reduction of pathogens (Fig. 5) despite the fact that the concentration of Ag was lesser than that of aqueous Av-AgNPs (Fig. 6). The NPs, whether immobilized or in suspension, were found to be most potent against *C. albicans*, as evident from the MIC (25 µg/mL) and MBC (50 µg/mL) values.

Owing to its antimicrobial properties against MDR pathogens, Av-Ag-FP was further assessed for its ability to eliminate/reduce *E. coli* present in water. A pronounced decrease in the CFU count was noted; the highest CFU reduction was ~70% in comparison

Table 1
Antibiotics resistance profile of selected pathogens.

Sr. No.	Antibacterial/antifungal drugs	Bacterial/fungal pathogens				
		<i>E. coli</i>	<i>A. baumannii</i>	<i>P. aeruginosa</i>	<i>S. aureus</i>	<i>C. albicans</i>
1	Ampicillin	R	S	R	S	–
2	Tetracycline	R	R	R	R	–
3	Gentamicin	S	R	R	PR	–
4	Streptomycin	R	PR	PR	S	–
5	Chloramphenicol	PR	S	R	S	–
6	Tigecycline	S	S	S	S	–
7	Trimethoprim sulfamethoxazole	R	PR	R	R	–
8	Fluconazole	–	–	–	–	–
9	Amphotericin B	–	–	–	–	S
Strain resistant against drugs		5/7	4/7	6/7	3/7	1/2

R, resistant; PR, partially resistant; S, sensitive.

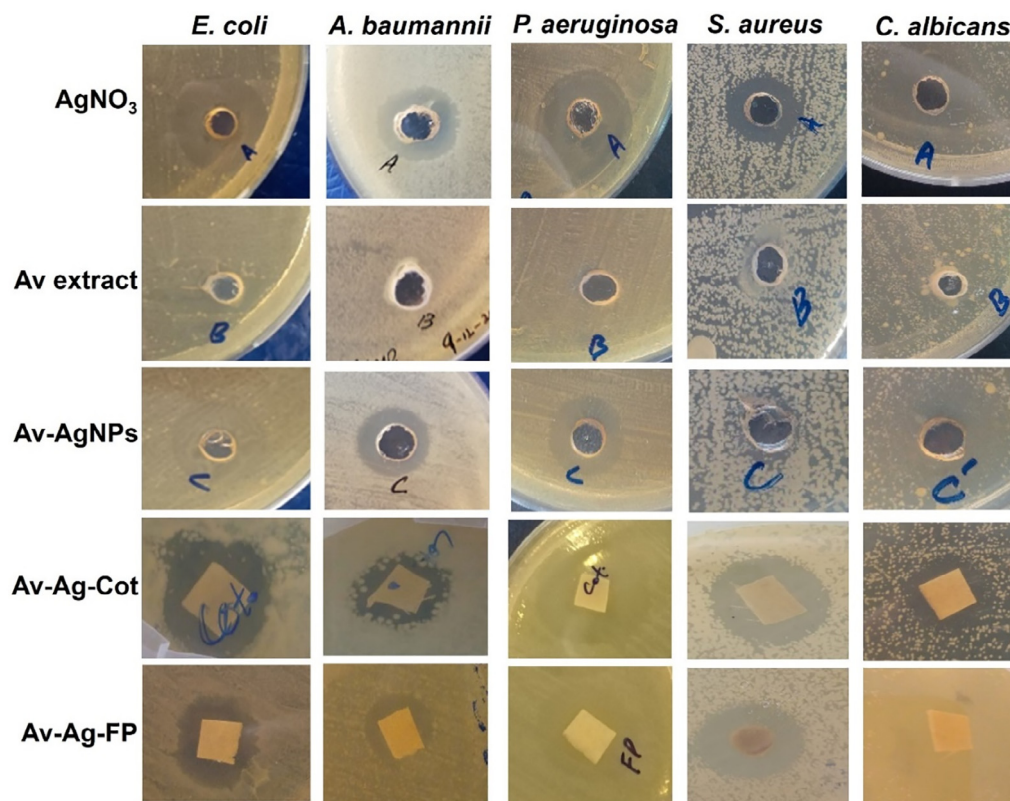


Fig. 5. Antimicrobial assay. Antibacterial action of AgNO₃, Av extract, Av-AgNPs, Av-Ag-Cot and Av-Ag-FP on Gram-negative (*E. coli*, *A. baumannii*, *P. aeruginosa*) and Gram-positive (*S. aureus*) bacteria and yeast (*C. albicans*). The zone of inhibition around the samples confirmed the antimicrobial effect of the NPs.

with controls (data not shown). The leaching of AgNPs from Av-Ag-FP when observed by ICP-OES was 0.002 mg/mL in the filtrate.

4. Discussion

Nanoscale materials, for instance nanoparticles, nanocomposites, nanoemulsions, nanotubes, nanofibers, nanodevices, show several differences in their chemical and biophysical properties when compared with their macroscale counterparts. One of the key differences lies in their size and surface area properties, which make them more useful for applications in the biological system, biosensing, biolabeling, diagnostic imaging and gene therapies [5,9].

Until now, several research groups have described the *in vitro* green synthesis of NPs using methods requiring: (i) room temper-

ature but extended time duration (24–72 h), (ii) microwave heat, (iii) sunlight exposure or iv) high-temperature (up to 120–200°C), etc., for the reduction and capping process to complete (Table 2). However, the biologically mediated synthesis of Ag-based, Av-fabricated NPs presented herein is a one-step process for the efficient synthesis of NPs (4–6 h; 65°C) without any agglomeration and loss of antimicrobial activity when observed after several months. This appears to be an effective way to deal with MDR pathogens i.e., the microbes that cannot be tackled with a single line of antibiotics and thereby pose serious threats to life. Although the high surface-to-volume ratio of the NPs allowed the fabrication/incorporation of ample functional ligands of Av (phytochemicals such as aoin, sugars, flavonoids and phenolic compounds), this in parallel, enabled the enhanced interactions and deeper accessibility of the synthesized Av-AgNPs for improved targeting of the microbes. Long-term stability of Av-AgNPs in terms of

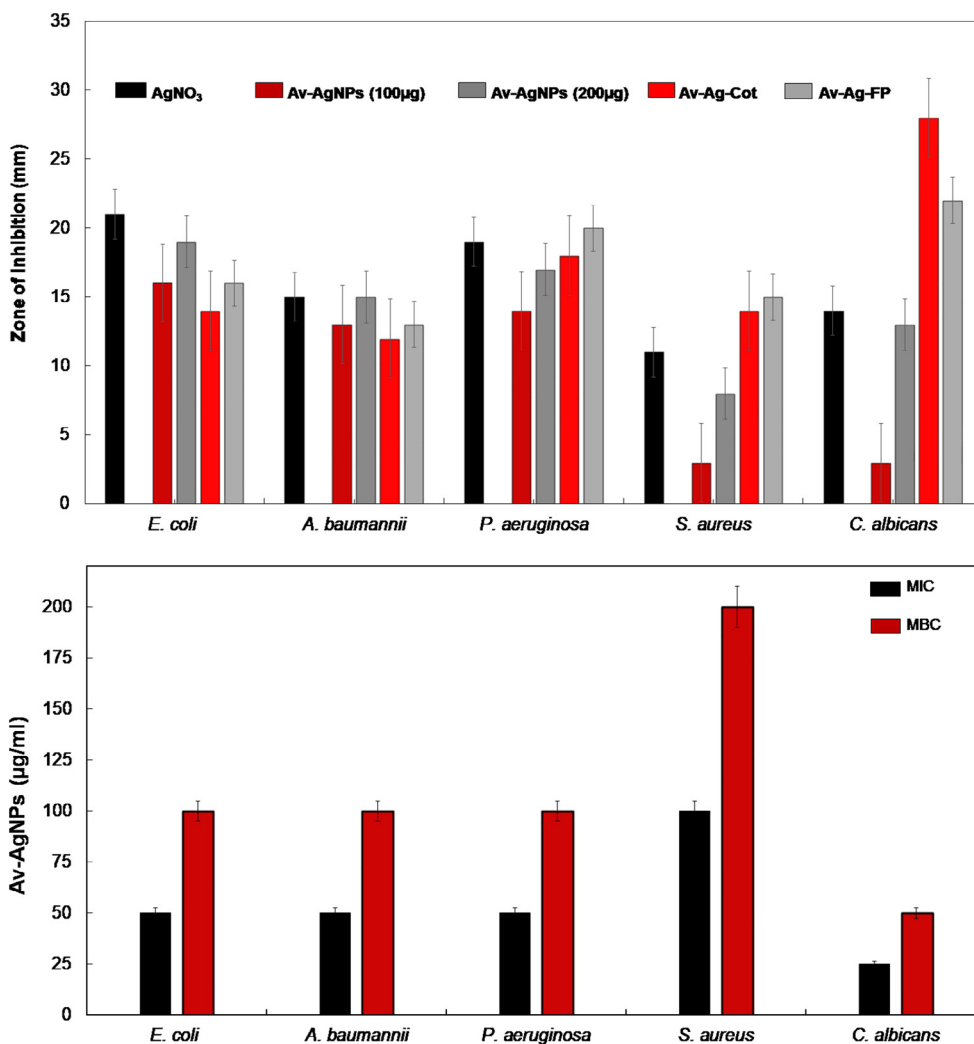


Fig. 6. Quantitative study for the antimicrobial effect. Antimicrobial evaluation of Soln. A, Soln. B, AvNPs (100 µg and 200 µg), Av-Ag-FP and Av-Ag-Cot on Gram-negative and Gram-positive bacteria and yeast. The well diffusion method and the Kirby Bauer method showed the inhibition in the form of clear zones (mm). The MIC and MBC for these MDR pathogens (*E. coli*, *A. baumannii*, *P. aeruginosa*, *S. aureus* and *C. albicans*) are depicted in columns. The highest MBC was confirmed for *S. aureus* (200 µg/ml), while the lowest MBC was observed for *C. albicans* (50 µg/ml).

dispersion at room temperature was made possible with thorough washing of the synthesized NPs with distilled water right after the synthesis step; the particles without washing were found to be agglomerated or aggregated – a phenomenon that could be due to the continuously occurring nucleation process. The Av-AgNPs synthesized in our study exhibited better homogenous shape and dispersion (Fig. 2, Fig. 4) compared with those reported in other studies [32,35].

Av-AgNPs exerted a promising antimicrobial effect against Gram-negative and -positive MDR bacteria and more importantly in case of fluconazole-resistant *C. albicans*. Although the exact mechanism by which NPs kill microorganisms is not known, there are various reports presenting the different possible modes of action of NPs [9]; the two most promising include: (i) direct release, penetration and accumulation of NPs in the negatively charged cell wall and/or cell membrane of bacteria resulting in damage/killing through cell lysis, (ii) production and increase of reactive oxygen species (ROS) followed by the inhibition of DNA replication or damage of the cellular DNA by inducing changes in the DNA repair system with resultant cell growth inhibition. It is anticipated that in the instant case, the synergistic activity of Av constituents and the AgNPs hinders the process of vital enzyme synthesis and phosphorus-containing molecules such as DNA,

whereas their electrostatic interactions with lipid membranes impact/loosen the cell membrane integrity, thus resulting in microbial cell death.

As shown in Fig. 4, all the tested samples except soln. B showed a significant reduction in the growth of all pathogens. Cellulosic materials impregnated with Av-AgNPs also confirmed their role as antimicrobial materials. High MIC and MBC concentrations under the given conditions may be due to resistance development in microorganisms as reported in some studies [33]; it may occur due to the increasing use of AgNPs in various fields, which ultimately mutate the DNA of the pathogens leading to more antibiotic and silver resistance [36]. The protective nature of Av-Ag-Cot against fungus (*C. albicans*) pathogen makes it promising for treating or preventing fungal infections and enables its use in clothing such as socks, wound dressings, etc. Our study further suggested that the presence of AvNPs on cellulosic material is more active than the presence of Ag ions alone, making the approach more eco-friendly for water purification applications.

The retention of silver NPs in the matrices of cellulosic material had been a challenge due to the weak forces such as H-binding and Van der Waals interactions between the NPs and the cellulosic material. The retention of metallic NPs also depends on the method of immobilization [33]. To avert leaching from the paper material,

Table 2
Comprehensive overview of the studies describing the synthesis and antimicrobial properties of *Aloe vera*-based AgNPs.

Reference	AgNO ₃ conc. (mM)	Other chemicals used	Plant extract (%; w/v)	Incubation temp./time	Shape	Size (nm)	Antimicrobial effect				
							Bacterial strain	Yeast/fungal strain	MIC	ZOI (mm)	NPs (ZOI) (µg/mL)
Chandran et al., 2006 [26]	01	NH ₄ OH	30	RT, 24 h	Spherical	15 ± 4	NA	NA	NA	NA	NA
Zhang et al., 2013 [28]	10	Nil	30	RT, 24 h	Spherical	25	<i>E. coli</i>	NA	200 µmol/ L	NA	NA
Zhang et al., 2013 [28]	01	Hydrazine	40	RT, 20 min	Spherical	20	<i>E. coli, S. aureus</i>	NA	NA	08	NA
Dinesh et al., 2015 [29]	01	Acetone	10	RT	Spherical	35–55	<i>B. subtilis, K. pneumoniae, S. typhi</i>	NA	NA	80–91	150
Logaranjan et al., 2016 [30]	10	NH ₄ OH, NaOH	NA	Microwave, 1 min	Octahedron	05–50	<i>S. aureus, B. cereus, M. luteus, E. coli, K. pneumoniae</i>	NA	NA	33–43	NA
Vélez et al., 2018 [31]	12	Ethanol	33 (leaf/gel)	57°C, 3 h 80°C, 2 h	Spherical	02–07 03–14	<i>Kocuria varians</i>	NA	40 µg/mL	NA	NA
Medda et al., 2015 [32]	10	Nil	10	RT, 72 h	Heterogeneous	70–293	NA	<i>Rhizopus & Aspergillus sp.</i>	22 ng/mL	NA	NA
Yuvasree et al., 2013 [36]	01	Nil	100 (gel)	RT, 24 h	NA	NA	<i>E. coli, Bacillus & Pseudomonas species</i>	NA	NA	08–11	NA
Moosa et al., 2015 [37]	1–10	Nil	10	RT, 10 min Sunlight	Spherical	34–102	NA	NA	NA	NA	NA
Rahman et al., 2017 [38]	1–4	Nil	30	65°C, 6 h	Spherical	12–200	NA	NA	NA	NA	NA
Yadav et al., 2016 [39]	01	Nil	20	RT, 24 h	Spherical	36 ± 4	<i>P. mirabilis, S. typhi, S. flexneri, S. aureus, E. coli, K. pneumoniae, P. aeruginosa</i>	NA	195–780	9–18	400–1000
Haripriya et al., 2017 [40]	01	Nil	30	RT, 24 h in dark	NA	–	<i>E. faecalis, S. mutans</i>	<i>C. albicans</i>	NA	14–38	500–2000
Khan et al., 2017 [41]	01	Nil	05	RT	Spherical	86–100	<i>E. coli, S. aureus, Salmonella, P. aeruginosa</i>	NA	05	0–16	20–120
Vineela et al., 2017 [42]	46	Nil	10	RT, 72 h	NA	NA	NA	NA	NA	NA	NA
Win et al., 2019 [43]	1–10	Nil	10	RT	NA	07–49	<i>B. cereus, S. aureus, E. coli, P. aeruginosa</i>	NA	NA	13–15	NA
Ahmadi et al., 2018 [44]	01	Nil	5	Microwave, 4–6 min	Spherical	46	<i>E. coli, S. aureus</i>	NA	NA	NA	NA
Dilshad et al., 2019 [45]	500	Nil	01 (gel)	RT, 30 min	Spherical	40 ± 4	<i>M. luteus, B. subtilis, E. aerogenes, A. tumefaciens, E. coli</i>	<i>A. niger, A. flavus, A. fumigatus, F. solani</i>	NA	06–19	05–100 for bacteria 250–1000 for fungi
This study	10	Nil	10	65°C ± 5, 4 h	Spherical	30–80	<i>E. coli, P. aeruginosa, A. baumannii, S. aureus</i>	<i>C. albicans</i>	25–100 µg/mL	08–19	100–200

RT, Room temperature (25°C); NA, information/data not available.

we have not used any chemical additive; the entrapment has been achieved due to the naturally present reducing and stabilizing agents of the Av extract. The leaching behavior of the Av-AgNPs impregnated on the filter paper was monitored by filtering distilled water and out of the two fractions collected (10 and 15 ml), the first filtrate contained ~ 0.0038 mg/ml silver while the second contained 0.0003 mg/ml silver. Thus, an average amount of Ag in 25 ml of filtered water was found to be equivalent to 2.0 $\mu\text{g/ml}$, which was remarkably lower than that reported earlier [37,38].

In the present study, the FP treated with soln. B also displayed a pronounced reduction in the bacterial CFU count. Although the pore size for Whatman FP is bigger (8–10 μm) than the *E. coli* cells (2–5 μm) but because of the attachment of the phytochemicals with the FP fibers, a mesh-like structure forms, which along with a slow flow rate (due to gravitational force) may contribute to the entrapment of *E. coli* and hence reduction in the bacterial CFUs. Overall, the performance of Av-Ag-FP was promising for water treatment but factors such as leaching of NPs, flow rate, durability of filter paper and filter design need special considerations in future studies. Recently, a good number of research groups have discussed the methodologies for the treatment of cotton fabric or other materials but using harmful chemicals and/or complex methodologies [28]; the present study presents an approach that is simpler and that eliminates the use of additional and harmful chemicals. The study is likely to widen the horizons of the antimicrobial applications of silver NPs in a broad range of biomedical applications.

5. Conclusions

In summary, this study led to the quick (4 h incubation at $65 \pm 5^\circ\text{C}$) and successful production of Av-AgNPs following an eco-friendly approach, i.e., without involving any harmful chemicals. Characterization of the materials using SEM, FTIR and ICP-OES confirmed the presence of spherical shaped, 30–80 nm sized, active Av-AgNPs, with the MIC ranging from 25 to 100 $\mu\text{g/ml}$ against bacterial and fungal pathogens. Their immobilization on cellulosic materials such as Av-Ag-Cot and Av-Ag-FP proved as potent for MDR bacterial and fungal pathogens, resulting in a significant reduction in the microbial growth. Av-Ag-FP exhibited a pronounced decrease in the *E. coli* CFUs in the filtrate when used for water purification. The method of immobilization, because of its non-toxicity and cost-effectiveness, has great scope for biomedical and environmental applications. Further studies using different materials for immobilization (e.g., surgical bandages used in wound healing) may be conducted for relevant biomedical applications.

Financial support

This study was partially supported by a grant from the University of the Punjab, Lahore, Pakistan.

Conflict of interest

All authors declare that they have no conflict of interest.

Data availability

All data generated or analyzed during this study are included in this published article.

References

- [1] Burnham JP, Olsen MA, Kollef MH. Re-estimating annual deaths due to multidrug-resistant organism infections. *Infect Control Hosp Epidemiol* 2019;40(1):112–3. <https://doi.org/10.1017/ice.2018.304>. PMID: 30463634.
- [2] Perdikouri EIA, Arvaniti K, Lathyris D, et al. Infections due to multidrug-resistant bacteria in oncological patients: Insights from a five-year epidemiological and clinical analysis. *Microorganisms* 2019;7(9):277. <https://doi.org/10.3390/microorganisms7090277>. PMID: 31438593.
- [3] Abadi ATB, Rizvanov AA, Haertlé T, et al. World Health Organization report: Current crisis of antibiotic resistance. *BioNanoSci* 2019;9:778–88. <https://doi.org/10.1007/s12668-019-00658-4>.
- [4] <https://www.who.int/news-room/fact-sheets/detail/antimicrobial-resistance>.
- [5] Gao W, Zhang L. Nanomaterials arising amid antibiotic resistance. *Nat Rev Microbiol* 2021;19(1):5–6. <https://doi.org/10.1038/s41579-020-00469-5>. PMID: 3302431.
- [6] Linklater DP, Baulin VA, Juodkazis S, et al. Mechano-bactericidal actions of nanostructured surfaces. *Nat Rev Microbiol* 2021;19(1):8–22. <https://doi.org/10.1038/s41579-020-0414-z>. PMID: 32807981.
- [7] Makabenta JMV, Nabawy A, Li CH, et al. Nanomaterial-based therapeutics for antibiotic-resistant bacterial infections. *Nat Rev Microbiol* 2021;19(1):23–36. <https://doi.org/10.1038/s41579-020-0420-1>. PMID: 32814862.
- [8] Shaikh S, Nazam N, Rizvi SMD, et al. Mechanistic insights into the antimicrobial actions of metallic nanoparticles and their implications for multidrug resistance. *Int J Mol Sci* 2019;20(10):2468. <https://doi.org/10.3390/ijms20102468>. PMID: 31109079.
- [9] Salleh A, Naomi R, Utami ND, et al. The potential of silver nanoparticles for antiviral and antibacterial applications: A mechanism of action. *Nanomaterials* 2020;10(8):1566. <https://doi.org/10.3390/nano10081566>. PMID: 32784939.
- [10] Lara HH, Ayala-Núñez NV, del Turrent LCI, et al. Bactericidal effect of silver nanoparticles against multidrug-resistant bacteria. *World J Microbiol Biotechnol* 2010;26:615–21. <https://doi.org/10.1007/s11274-009-0211-3>.
- [11] Fayaz AM, Balaji K, Girilal M, et al. Biogenic synthesis of silver nanoparticles and their synergistic effect with antibiotics: A study against gram-positive and gram-negative bacteria. *Nanomedicine* 2010;6(1):103–9. <https://doi.org/10.1016/j.nano.2009.04.006>. PMID: 19447203.
- [12] Guzman M, Dille J, Godet S. Synthesis and antibacterial activity of silver nanoparticles against gram-positive and gram-negative bacteria. *Nanomed Nanotechnol Biol Med* 2012;8(1):37–45. <https://doi.org/10.1016/j.nano.2011.05.007>. PMID: 21703988.
- [13] Venkatadri B, Shanparvish E, Rameshkumar MR, et al. Green synthesis of silver nanoparticles using aqueous rhizome extract of *Zingiber officinale* and *Curcuma longa*: In-vitro anti-cancer potential on human colon carcinoma HT-29 cells. *Saudi J Biol Sci* 2020;27(11):2980–6. <https://doi.org/10.1016/j.sjbs.2020.09.021>. PMID: 33100856.
- [14] Ganesan RM, Prabu HG. Synthesis of gold nanoparticles using herbal *Acorus calamus* rhizome extract and coating on cotton fabric for antibacterial and UV blocking applications. *Arab J Chem* 2019;12(8):2166–74. <https://doi.org/10.1016/j.arabic.2014.12.017>.
- [15] Ahmad T, Bustam MA, Irfan M, et al. Mechanistic investigation of phytochemicals involved in green synthesis of gold nanoparticles using aqueous *Elaeis guineensis* leaves extract: Role of phenolic compounds and flavonoids. *Biotechnol Appl Biochem* 2019;66(4):698–708. <https://doi.org/10.1002/bab.1787>. PMID: 31172593.
- [16] Mukherjee P, Ahmad A, Mandal D, et al. Fungus-mediated synthesis of silver nanoparticles and their immobilization in the mycelial matrix: A novel biological approach to nanoparticle synthesis. *Nano Lett* 2001;1(10):515–9. <https://doi.org/10.1021/nl0155274>.
- [17] Ali M, Ahmed T, Wu W, et al. Advancements in plant and microbe-based synthesis of metallic nanoparticles and their antimicrobial activity against plant pathogens. *Nanomaterials* 2020;10(6):1146. <https://doi.org/10.3390/nano10061146>. PMID: 32545239.
- [18] Gopinath K, Kumaraguru S, Bhakayaraj K, et al. Green synthesis of silver, gold and silver/gold bimetallic nanoparticles using the *Gloriosa superba* leaf extract and their antibacterial and antibiofilm activities. *Microb Pathog* 2016;101:1–11. <https://doi.org/10.1016/j.micpath.2016.10.011>. PMID: 27765621.
- [19] Shankar SS, Rai A, Ahmad A, et al. Rapid synthesis of Au, Ag, and bimetallic Au core–Ag shell nanoparticles using Neem (*Azadirachta indica*) leaf broth. *J Colloid Interface Sci* 2004;275(2):496–502. <https://doi.org/10.1016/j.jcis.2004.03.003>. PMID: 15178278.
- [20] Alti D, Rao MV, Rao DN, et al. Gold–silver bimetallic nanoparticles reduced with herbal leaf extracts induce ROS-mediated death in both promastigote and amastigote stages of *Leishmania donovani*. *ACS Omega* 2020;5(26):16238–45. <https://doi.org/10.1021/acsomega.0c02032>. PMID: 32656446.
- [21] Nguyen DH, Lee JS, Park KD, et al. Green silver nanoparticles formed by *Phyllanthus urinaria*, *Pouzolzia zeylanica*, and *Scoparia dulcis* leaf extracts and the antifungal activity. *Nanomaterials* 2020;10(3):542. <https://doi.org/10.3390/nano10030542>. PMID: 32192177.
- [22] Unuofin JO, Oladipo AO, Msagati TAM, et al. Novel silver-platinum bimetallic nanoalloy synthesized from *Vernonia mespilifolia* extract: Antioxidant, antimicrobial, and cytotoxic activities. *Arab J Chem* 2020;13(8):6639–48. <https://doi.org/10.1016/j.arabic.2020.06.019>.

- [23] Sharma C, Ansari S, Ansari MS, et al. Single-step green route synthesis of Au/Ag bimetallic nanoparticles using clove buds extract: Enhancement in antioxidant bio-efficacy and catalytic activity. *Mater Sci Eng C* 2020;116(8):111153. <https://doi.org/10.1016/j.msec.2020.111153>. PMID: 32806256.
- [24] Khan M, Al-hamoud K, Liaqat Z, et al. Synthesis of Au, Ag, and Au–Ag bimetallic nanoparticles using *Pulicaria undulata* extract and their catalytic activity for the reduction of 4-nitrophenol. *Nanomaterials* 2020;10(9):1885. <https://doi.org/10.3390/nano10091885>.
- [25] Saniasiy J, Salim R, Mohamad I, et al. Antifungal effect of Malaysian *Aloe vera* leaf extract on selected fungal species of pathogenic otomycosis species in in vitro culture medium. *Oman Medical J* 2017;32(1):41–6. <https://doi.org/10.5001/omj.2017.08>. PMID: 28042402.
- [26] Chandran SP, Chaudhary M, Pasricha R, et al. Synthesis of gold nanotriangles and silver nanoparticles using *Aloe vera* plant extract. *Biotechnol Prog* 2006;22(2):577–83. <https://doi.org/10.1021/bp0501423>. PMID: 16599579.
- [27] Tippayawat P, Phromviyo N, Boueroy P, et al. Green synthesis of silver nanoparticles in *Aloe vera* plant extract prepared by a hydrothermal method and their synergistic antibacterial activity. *PeerJ* 2016;4:e2589. <https://doi.org/10.7717/peerj.2589>.
- [28] Zhang Y, Cheng X, Zhang Y, et al. Biosynthesis of silver nanoparticles at room temperature using aqueous aloe leaf extract and antibacterial properties. *Colloids Surf, A* 2013;423:63–8. <https://doi.org/10.1016/j.colsurfa.2013.01.059>.
- [29] Dinesh D, Murugan K, Madhiyazhagan P, et al. Mosquitocidal and antibacterial activity of green-synthesized silver nanoparticles from *Aloe vera* extracts: Towards an effective tool against the malaria vector *Anopheles stephensi*. *Parasitol Res* 2015;114(4):1519–29. <https://doi.org/10.1007/s00436-015-4336-z>. PMID: 25653031.
- [30] Logaranjan K, Raiza AJ, Gopinath SC, et al. Shape- and size-controlled synthesis of silver nanoparticles using *Aloe vera* plant extract and their antimicrobial activity. *Nanoscale Res Lett* 2016;11(1). <https://doi.org/10.1186/s11671-016-1725-x>. PMID: 27885623.
- [31] Vélez E, Campillo G, Morales G, et al. Silver nanoparticles obtained by aqueous or ethanolic *Aloe vera* extracts: An assessment of the antibacterial activity and mercury removal capability 7215210. *J Nanomater* 2018. <https://doi.org/10.1155/2018/7215210>.
- [32] Medda S, Hajra A, Dey U, et al. Biosynthesis of silver nanoparticles from *Aloe vera* leaf extract and antifungal activity against *Rhizopus* sp. and *Aspergillus* sp.. *Appl Nanosci* 2015;5(7):875–80. <https://doi.org/10.1007/s13204-014-0387-1>.
- [33] Praveena SM, Han LS, Than LTL, et al. Preparation and characterisation of silver nanoparticle coated on cellulose paper: Evaluation of their potential as antibacterial water filter. *J Exp Nanosci* 2016;11(17):1307–19. <https://doi.org/10.1080/17458080.2016.1209790>.
- [34] Sathvika K, Rajeshkumar S, Roy A, et al. Antibacterial activity of silver nanoparticles mediated *Aloe vera* with neem against dental pathogens. *Ind J Pub Health Res Develop* 2019;10(11):3469. <https://doi.org/10.5958/0976-5506.2019.04120.2>.
- [35] Selvakumar PM, Antonyraj CA, Babu R, et al. Green synthesis and antimicrobial activity of monodispersed silver nanoparticles synthesized using lemon extract. *Synth React Inorg, Met-Org, Nano-Met Chem* 2016;46(2):291–4. <https://doi.org/10.1080/15533174.2014.971810>.
- [36] Yuvasree P, Nithya K, Neelakandeswari N. Biosynthesis of silver nanoparticles from *Aloe vera* plant extract and its antimicrobial activity against multidrug resistant pathogens. *ICANMEET* 2016;3:84–86. <https://doi.org/10.1109/ICANMEET.2013.6609241>.
- [37] Moosa AA, Ridha AM, Al-Kaser M. Process parameters for green synthesis of silver nanoparticles using leaves extract of *Aloe vera* plant. *IJMRC* 2015;3:966–75.
- [38] Rahman A, Rashid A, Antor MAA, et al. Green synthesis and characterization of silver nanoparticles by using *Aloe vera* leaf extract to study the effects of synthesis parameters. *Appl Mech Mater* 2016;860:179–84. <https://doi.org/10.4028/www.scientific.net/AMM.860.179>.
- [39] Yadav J, Kumar S, Budhwar L, et al. Characterization and antibacterial activity of synthesized silver and iron nanoparticles using *Aloe vera*. *J Nanomed* 2016;7:384. <https://doi.org/10.4172/2157-7439.1000384>.
- [40] Haripriya S, Ajitha P. Antimicrobial efficacy of silver nanoparticles of *Aloe vera*. *J Adv Pharm Edu Res* 2017;7(2):163–7.
- [41] Khan A, Shaheen A, Mahmood T, et al. Novel synthesis and characterization of silver nanoparticles from leaf aqueous extract of *Aloe vera* and their antimicrobial activity. *J Nanosci Nanotechnol Appl* 2017;1(1):103.
- [42] Vineela D, Reddy SJ, Kumar KB. Synthesis of silver nanoparticles by using *Aloe vera* leaf extract for growth enhancement of fish *Catla catla*. *World J Pharm Med Res* 2017;3(3):93–7.
- [43] Win SS, Shwe H, Su BHC, et al. Synthesis and characterization of silver nanoparticles using leaves extract of *Aloe vera* (L.) Burm. f. *IEEE-SEM*. 2019;7(7):75–83.
- [44] Ahmadi O, Jafarizadeh-Malmiri H, Jodeiri N. Eco-friendly microwave-enhanced green synthesis of silver nanoparticles using *Aloe vera* leaf extract and their physico-chemical and antibacterial studies. *Green Proc Synth* 2018;7(3):231–40. <https://doi.org/10.1515/gps-2017-0039>.
- [45] Dilshad E, Tazeem SS, Bashir Z, et al. Silver nanoparticles of *Aloe vera* gel as strong therapeutic candidates. *IJB* 2019;15(1):360–73.